Micron 204 (2026) 104018

Contents lists available at ScienceDirect

Micron

journal homepage: www.elsevier.com/locate/micron

The first analysis of the sperm ultrastructure of Mycetophagidae, Tetratomidae, and mycetophagous Tenebrionidae (Coleoptera: Tenebrionoidea)

David Mercati [a], Jan Batelka [b], Mariangela Gentile [a], Pietro Lupetti [a], Romano Dallai [a,*]

[a] Department of Life Sciences, University of Siena, Siena, Italy
[b] Nad vodovodem 16, Praha 10, Czech Republic

ARTICLE INFO

Keywords:
Insect sperm ultrastructure
Beetle phylogeny
Tenebrionoidea relationships

ABSTRACT

Tenebrionoidea, a diverse beetle superfamily, exhibits complex and poorly resolved phylogenetic relationships. Sperm ultrastructure varies notably among its families, yet many remain unstudied. Here we examined for the first time the sperm morphology in four species from the families Mycetophagidae, Tetratomidae, and Tenebrionidae using ultrastructural techniques. We observed a consistent antiparallel arrangement of spermatids or spermatozoa in the germ cysts and documented significant interspecific differences in acrosome and nucleus dimensions. Flagellar analyses revealed asymmetrical mitochondrial derivatives and an unprecedented tail-end microtubule arrangement. These findings refine species identification and enhance understanding of reproductive morphology within Tenebrionoidea. Our results underscore the utility of sperm ultrastructure as a taxonomic and phylogenetic tool, highlighting its potential to clarify evolutionary relationships in this complex group, while also indicating the necessity for further studies encompassing additional species.

1. Introduction

Tenebrionoidea is among the most numerous and complex superfamilies within Cucujformia (Crowson, 1966; Lawrence and Newton, 1995; Lawrence et al., 2011; Robertson et al., 2015; Beutel and Friedrich, 2005; Bouchard et al., 2021). However, the monophyly of this superfamily is not well supported. Despite increasing efforts to recover the phylogenetic relationships of families and genera within Tenebrionoidea using Next Generation Sequencing (NGS) methods, the knowledge is still only fragmentary.

Tetratoma is absent in Kergoat et al. (2014), Tetratomidae are polyphyletic in both subclades of Tenebrionoidea. Mycetophagidae (*Mycetophagus* + *Litargus* + *Litophagus*) are sister to Tetratomidae (*Synstrophus*). *Neomida* and *Bolitophagus* were not sampled. In Zhang et al. (2018) Mycetophagidae (*Mycetophagus* + *Nototriphyllus*) are placed in clade sister to Archaeocrypticidae + Ulodidae. Tetratomidae, *Neomida* and *Bolitophagus* are absent. McKenna et al. (2019) sampled from Tetratomidae the genus *Hallomenus*, which was recovered in the sister position to *Litargus* (Mycetophagidae). Sampling of Tenebrionidae was limited to three genera only including *Neomida*.Cai et al. (2022) recovered Mycetophagidae (*Mycetophagus* + *Nototriphyllus*) sister to Archaeocrypticidae. Tetratomidae, *Neomida* and *Bolitophagus* were not sampled. Hu et al. (2024) recovered *Tetratoma* sister to *Trictenotoma* (Trictenotomidae) in ML analysis, or to *Prostomis* (Prostomidae) using Bayesian methods. Mycetophagidae, *Neomida* and *Bolitophagus* were not sampled. Batelka et al. (2025a) analysed *M. quadripustulatus*, *T. fungorum* and *Neomida bicornis*. In their ML analysis Mycetophagidae (*Mycetophagus* + *Litargus*) are sister to Tetratomidae (*Tetratoma* + *Hallomenus*), sampling of Tenebrionidae was limited to three genera only.

Studies of sperm structure in Tenebrionoidea families have revealed important differences in the length and shape of sperm components, such as the acrosome, nucleus, and details of the flagellar structure, particularly the shape and diameter of the mitochondrial derivatives and accessory bodies (Baccetti et al., 1973; Afzelius and Dallai, 1994; Jamieson et al., 1999; Dallai, 2014). A notable feature, recently described in several Tenebrionoidea families, is the antiparallel arrangement of spermatids within cysts during spermiogenesis, with nuclei migrating toward opposite apical regions of the cysts—a pattern clearly detected by nuclear fluorescence staining (Dias et al., 2012).

* Corresponding author.
E-mail addresses: david.mercati@unisi.it (D. Mercati), janbat@centrum.cz (J. Batelka), mariangela.gentile@unisi.it (M. Gentile), pietro.lupetti@unisi.it (P. Lupetti), romano.dallai@unisi.it (R. Dallai).

https://doi.org/10.1016/j.micron.2026.104018
Received 16 January 2026; Received in revised form 6 March 2026; Accepted 21 March 2026
Available online 21 March 2026

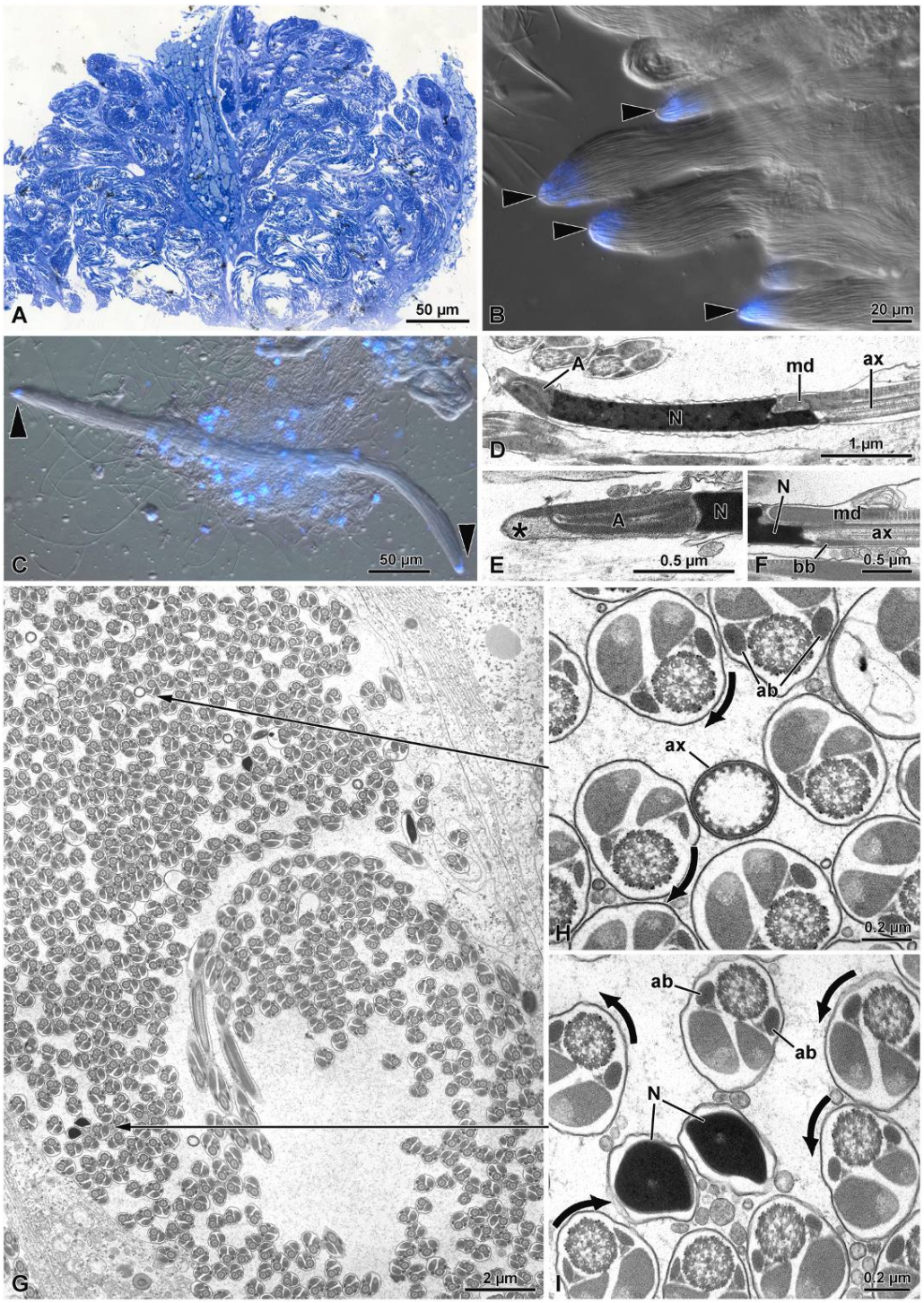

Fig. 1. *Bolitophagus reticulatus*. A) Semithin section of a follicle showing numerous sperm cysts with sperm bundles bent due to the sperm length. B, C) Hoechst staining of sperm bundles with antiparallel position. Note the apical nuclei and their opposite position (arrowheads). D, E) Longitudinal sections of the head region with the short nucleus (N) and the acrosome (A) with an apical extension (asterisk). ax, axoneme; md, mitochondrial derivative. F) Longitudinal section of the posterior nuclear region (N) showing the basal body (bb) and the axoneme (ax) on a side and the mitochondrial derivatives (md) on the opposite side. G-I) Cross sections through a sperm cyst showing in the two details (Figs H and I) the opposite axonemal orientation of flagella of the two antiparallel sperm bundles (see arrows). Note in H the particular structure of the axonemal end (ax) and in I the nuclear shape (N). ab, accessory bodies.

More recently, morphological and molecular data have established a new "Mordelloid clade" within Tenebrionoidea, comprising the families Mordellidae and Ripiphoridae (Batelka et al., 2025a). Member of this clade possess unique morphological characteristics but lack the antiparallel sperm arrangement that is typical of other Tenebrionoidea families studied to date (Dias et al., 2015a, b, 2021, 2022a, b; Folly et al., 2021; Rezende et al., 2024a, b; Batelka et al., 2026). To date, sperm ultrastructure has been described for only six of more than 30 identified families within the superfamily Tenebrionoidea (Ciidae, Meloidae, Oedemeridae, Pythidae, Scraptiidae, and Tenebrionidae; for review see Batelka et al., 2026). The present work aims to further expand our understanding of Tenebrionoidea evolution by investigating the sperm

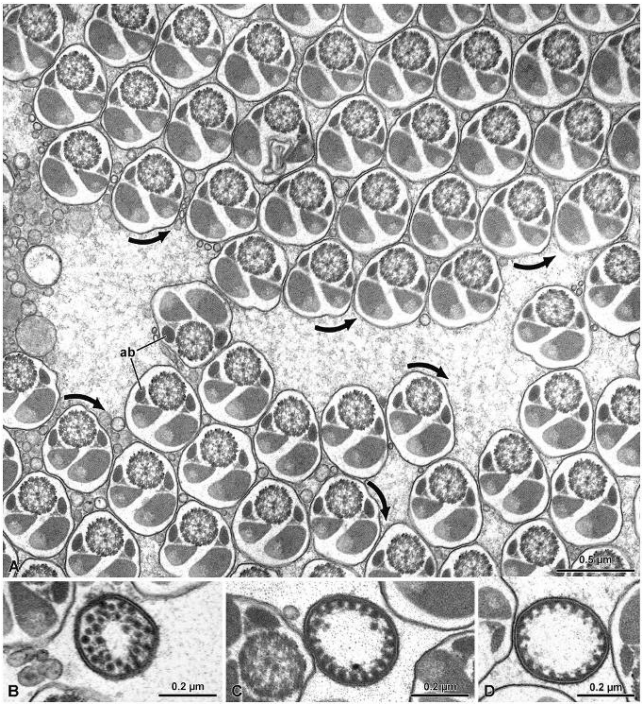

Fig. 2. *Bolitophagus reticulatus*. A) Cross section through the two antiparallel bundles at half of their length. Note the opposite orientation (see arrows) of their axoneme. ab, accessory bodies. B-D) Cross sections at three different levels of the tail end showing the progressive axoneme modification. At the tail tip all microtubules are beneath the plasma membrane.

ultrastructure of four species belonging to Mycetophagidae, Tetratomidae, and mycetophagous representatives of Tenebrionidae.

2. Material and methods

All specimens have been collected in the Czech Republic and identified by J. Batelka.

Mycetophagidae: *Mycetophagus quadripustulatus* (Linnaeus, 1760); 30 km E of Praha, Jevany env. September 2025, on fungus *Pleurotus pulmonarius*.

Tetratomidae: *Tetratoma fungorum* Fabricius, 1790; 25–30 km E of Praha, Vyžlovka env. and Jevany env. October 2025, on fungus *Pleurotus pulmonarius*.

Tenebrionidae: *Bolitophagus reticulatus* (Linnaeus, 1767); 30 km E of Praha, Jevany env. September 2025, in fungus *Fomes fomentarius*.

Tenebrionidae: *Neomida haemorrhoidalis* (Fabricius, 1787); 30 km E of Praha, Jevany env. September 2025, in fungus *Fomes fomentarius.*

2.1. Light microscopy (LM)

The male reproductive systems of the four examined species were isolated by dissection in 0.1 M phosphate buffer (pH 7.2) supplemented with 3% sucrose (PB). The specimens were then transferred onto a microscope slide in a small drop of PB. For fluorescence observations, DNA was stained by incubating the material for 3–4 min in 1 µg/ML Hoechst 33258 (Sigma) in PB. Samples were observed and photographed using differential interference contrast (DIC) and epifluorescence microscopy. Observations were performed with a Leica DMRB microscope equipped with an AxioCam HR camera (Carl Zeiss).

2.2. Transmission electron microscopy (TEM)

Males reproductive organs were dissected in PB and fixed overnight in 2.5% glutaraldehyde in PB at 4 °C. The material was carefully rinsed in PB and post-fixed in 1% osmium tetroxide in PB for 2 h. Subsequently, the samples were washed in PB and dehydrated through a graded ethanol series (50–100%). The material was then transferred into propylene oxide and embedded in an Epon-Araldite resin mixture. After polymerization at 60 °C for 48 h, the blocks were sectioned using a Diatome diamond knife on a Reichert Ultracut II E ultramicrotome. Semithin sections were mounted on glass slides, stained with 1% toluidine blue, and examined under a Leica DMRB microscope using differential interference contrast (DIC). Ultrathin sections were routinely stained with uranyl acetate and lead citrate and examined with a Philips CM10 electron microscope operating at 80 kV.

3. Results

3.1. Bolitophagus reticulatus (Tenebrionidae)

The testis follicles are filled with long sperm cysts. In areas where the cysts are less compact and the sperm bundles are relaxed, semi-thin sections reveal the sinuous nature of the sperm bundles (Fig. 1A). After fluorescence staining, it is observed that both ends of the cysts show marking, indicating that the spermatozoa in each germinal cyst are arranged in an antiparallel orientation (Fig. 1B, C). Higher magnification of the distal regions of these sections shows that the flagellar axonemes are oriented in opposite directions (Fig. 1G-I). The sperm are approximately 224 µm long and possess an acrosome (0.93 µm) with a perforatorium and an apical expansion about 0.25 µm long, filled with moderately electron-dense material (Fig. 1D-E), resulting in a three-layered acrosome. The nucleus is elliptical in cross section (Fig. 1I) and notably short (2.10 µm), characterized by highly compact chromatin (Fig. 1D). Posteriorly, it extends on one side in continuity with the basal body and axoneme, while on the opposite side it houses a large mitochondrial derivative (Fig. 1D, F). The flagellum is long and contains a $9+9+2$ axoneme with electron-dense accessory tubules. Two unequal mitochondrial derivatives are present; the one on the left side of the axoneme is thicker than the one on the right (Figs. 1H, I; 2A). However, at about half the flagellar length, the two mitochondria are nearly identical in diameter. The matrix of the mitochondrial derivatives facing the axoneme is denser than the opposite region (Figs. 1H, I; 2A). Two small, elliptical accessory bodies (0.11 µm × 46 nm) are located lateral to the axoneme (Figs. 1H, I; 2A). Toward the tail end, only one mitochondrial derivative remains visible before it disappears, leaving only the axoneme. Later, the axoneme becomes disorganized, and all microtubular elements are arranged beneath the plasma membrane, forming an unusual structure (Fig. 2B-D).

3.2. Neomida haemorrhoidalis (Tenebrionidae)

Testes have follicles with germ cysts filled with bundles of long, sinuous perm cells (Fig. 3A). The spermatozoa are arranged in an antiparallel orientation within the cysts (Fig. 3B). Sperm are about 180 µm long, and each sperm bundle consists of about 500 sperm units, thus the species has germ cysts with $2^{10} = 1024$ sperm. The sperm has an apical acrosome showing at its anterior region a long expansion apparently empty (Fig. 4A, B). Early spermatids show spheroidal acrosomes, 0.85 µm in diameter, adherent to the nuclear apex (Fig. 3C). Upon maturity, the acrosome reaches about 1.43 µm of length (Fig. 4B). The cylindrical nucleus is about 7.60 µm long and 0.4 µm in diameter (Fig. 3D, E; 4B-C). Apically, it tapers to a reduced diameter and an elliptical shape (Fig. 4A). In young spermatids, the nuclei are ovoid (2.5 µm long × 1.85 µm wide). Posteriorly, the nucleus is modified to accommodate the basal body and flagellar axoneme on one side, and a mitochondrial derivative on the opposite side (Fig. 4C). A cross section through this nuclear region clearly shows that the nucleus has a semilunar shape and it hosts a few microtubules of the initial axoneme (Fig. 4 inset). On the opposite nuclear side, a mitochondrial derivative is apparent (Fig. 4C). The flagellum displays the typical $9+9+2$

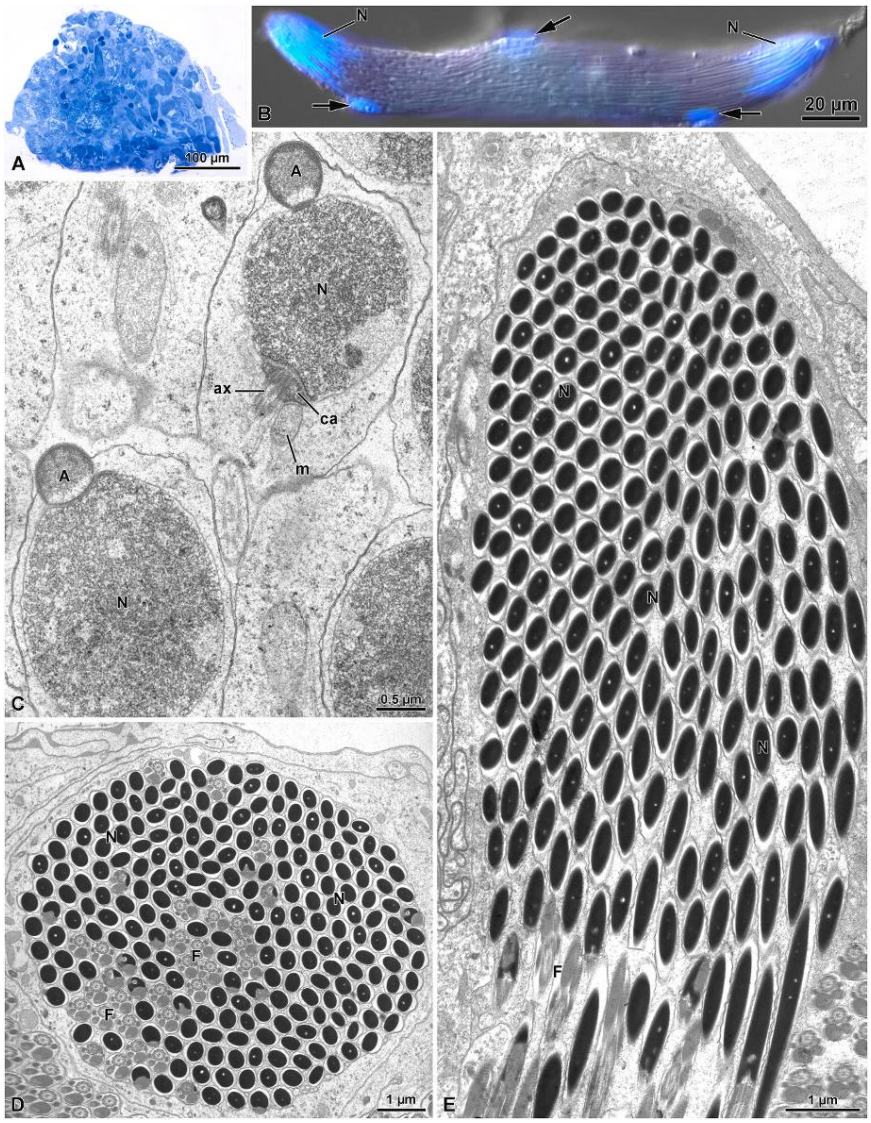

Fig. 3. *Neomida haemorrhoidalis*. A) Semithin section of a follicle showing the numerous sperm cysts. B) Hoechst staining of a sperm bundle in an antiparallel position. The nucleus (N) are on the apical position at the two opposite extremities of the sperm bundle. Note also the nuclei of the sperm cyst (arrows). C) Cross section of early spermatids with the apical roundish acrosome (A) and the ovoidal nucleus (N). In the posterior nuclear region, the electron-dense material of the centriole adjunct (ca), the axoneme (ax) and a mitochondrion (m) are visible. D, E) Cross and longitudinal sections of a sperm bundle with about 500 sperm cells. Note the elliptical nuclei (N) and the initial flagellar region (F).

axoneme configuration. Opposite to the axoneme, two mitochondrial derivatives are present. That on the right side is larger than the opposite one, and it has an almost roundish cross section. The smaller mitochondrial derivative is about 1/3 of the larger one (Fig. 4C, D). The matrix of the two mitochondrial derivatives is denser towards the axonemal side. Two small globular accessory bodies (about only 62 nm each) are positioned lateral to the axoneme (Fig. 4C, D). Towards the tail end a single mitochondrial derivative is evident. At the tail end, which is only 0.2 µm wide, the axoneme appears disorganized, with all the microtubules just below the plasma membrane (Fig. 4E)

3.3. *Mycetophagus quadripustulatus (Mycetophagidae)*

The male reproductive apparatus of this species consists of two testes with 18–21 follicles each (Fig. 5A). Each follicle is pear-shaped, measuring 628 µm in length and 348 µm in width (Fig. 5B), and contains numerous fusiform germ cysts (Fig. 5D). After fluorescence treatment, the spermatozoa within each cyst are arranged in an antiparallel orientation (Fig. 5E). The follicle roundish apical region contains germ cysts with early stages of spermatogenesis, while the opposite pointed region has cysts filled with sperm bundles intermingled with large globular bodies, 0.3 µm in diameter, possible remnants of cyst degeneration (Figs. 5C; 8A, B). In the apical region of spermatocytes, ovoid nuclei show a synaptonemal complex (Fig. 6A); early spermatids are also commonly found (Fig. 6A-F). Large Golgi apparatuses are visible close to the apical nuclear region (Fig. 6A). In the early spermatid a centriole surrounded by electron-dense material of the centriole adjunct is present (Fig. 6B). Further, the spermatids have nuclei exhibiting the early stage of chromatin condensation, characterized by the presence of two electron-dense ribbons on two opposite nuclear sides (Fig. 6C). The flagellar axoneme is present with a $9 + 9 + 2$ microtubular pattern (Fig. 6D, E). Lateral to the axoneme two long mitochondrial derivatives, still provided with cristae are visible. At almost spermatid maturity, two small accessory bodies are visible and the mitochondrial derivatives show an electron-dense material in their matrix (Fig. 6F). The sperm are long, and show an apical acrosome, 0.82 µm long with an inner perforatorium and a short electron-dense elliptical tip (Fig. 7B). The nucleus is about 5.70 µm long and has an elliptical outline, in cross section

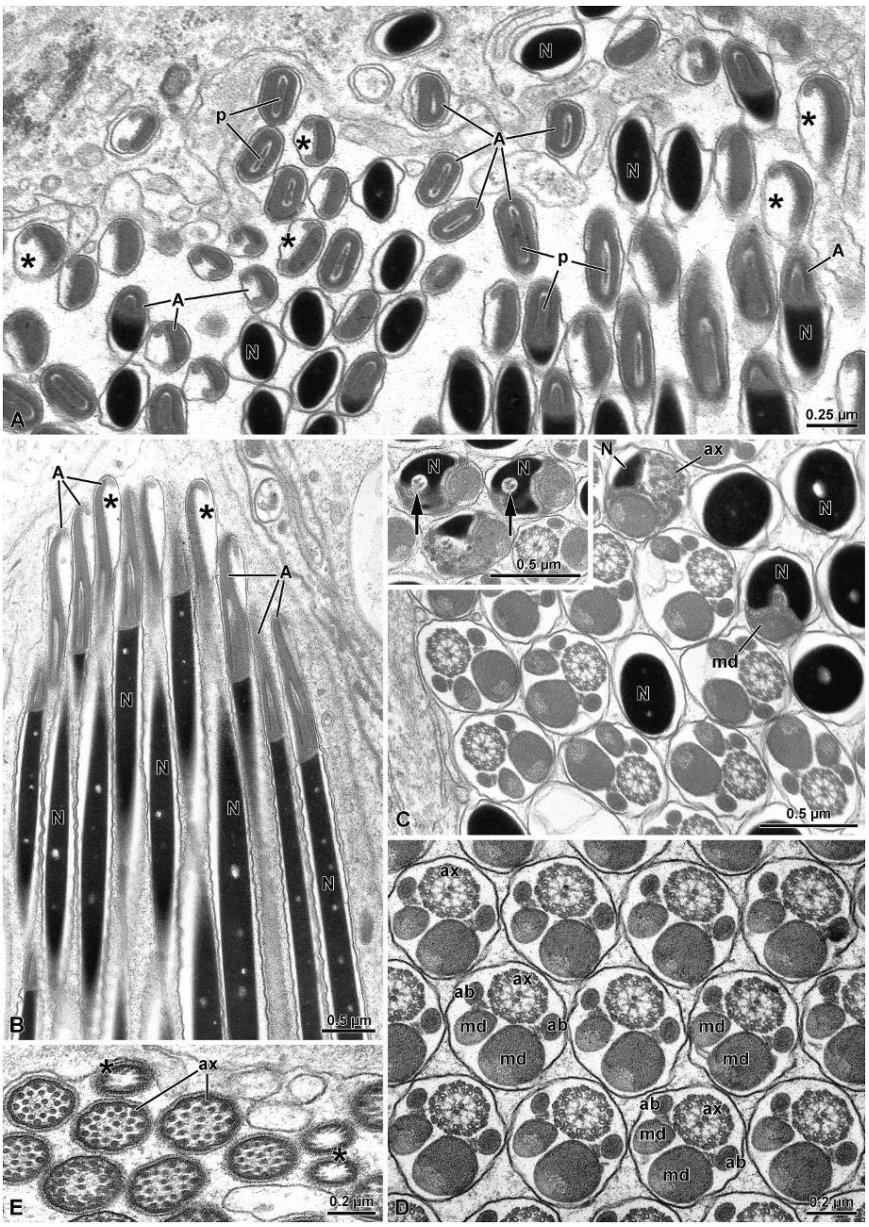

Fig. 4. *Neomida haemorrhoidalis*. A) Cross section through the sperm head region with the acrosome (A), showing the apical extension (asterisks) and the perforatorium (p), and the elliptical nuclei (N). B) Longitudinal section of sperm with the acrosome (A), with the apical extension (asterisks), and the nucleus (N). C) Cross section of the posterior nuclear region with a semilunar section (N), a single mitochondrial derivatives (md) and the beginning of the axoneme (ax). Note, in the inset, the presence of two microtubules in the nuclear axis (arrows). D) Cross section through the flagellar axoneme (ax) with the asymmetric mitochondrial derivatives (md) and the two ovoidal accessory bodies (ab). **E)** Cross section of the tail end with the disorganized axoneme (ax). Note the reduced section of the tail tip with microtubules beneath the plasma membrane (asterisks).

(0,34 µm × 0,27 µm) (Fig. 7A, C). Posteriorly, the nucleus has a deep cavity into which a mitochondrial derivative is on a side together with two small accessory bodies (Fig. 7B), while on the opposite side the two central axonemal tubule are present. A little behind the complete axoneme is apparent. Further posteriorly, the two mitochondrial derivatives are visible. The axoneme consists of a 9 + 9 + 2 microtubular pattern with electron-dense accessory tubules. Beneath two unequal mitochondrial derivatives are present. That on left side is larger than the opposite one (Fig. 7C, D). Two small elliptical or slightly spherical accessory bodies are lateral to the axoneme (Fig. 7C, D). A cross section through the sperm bundle within a cyst clearly shows that the sperm axonemes, as expected, have an opposite orientation; they are, in fact, a bundle with sperm arranged in an antiparallel orientation. (Fig. 7D). Towards the posterior end, the two mitochondrial derivatives gradually taper until one disappears, while the other persists. At the tail tip, only the axoneme remains; following the termination of the central microtubule pair (Fig. 7C, insets), the remaining microtubules reorganize just beneath the plasma membrane, forming an unusual peripheral configuration ().

3.4. *Tetratoma fungorum (Tetratomidae)*

The specimen examined displays a male reproductive apparatus that apparently has not evident testes (Fig. 9A). It is possible that, after completing spermiogenesis in a previous developmental instar, the male regresses its exhausted testes, with all sperm now contained in the large, sinuous deferent ducts (Fig. 9A, B). The sperm are long and possess a short acrosome (0.31 µm), which is flattened in cross section and

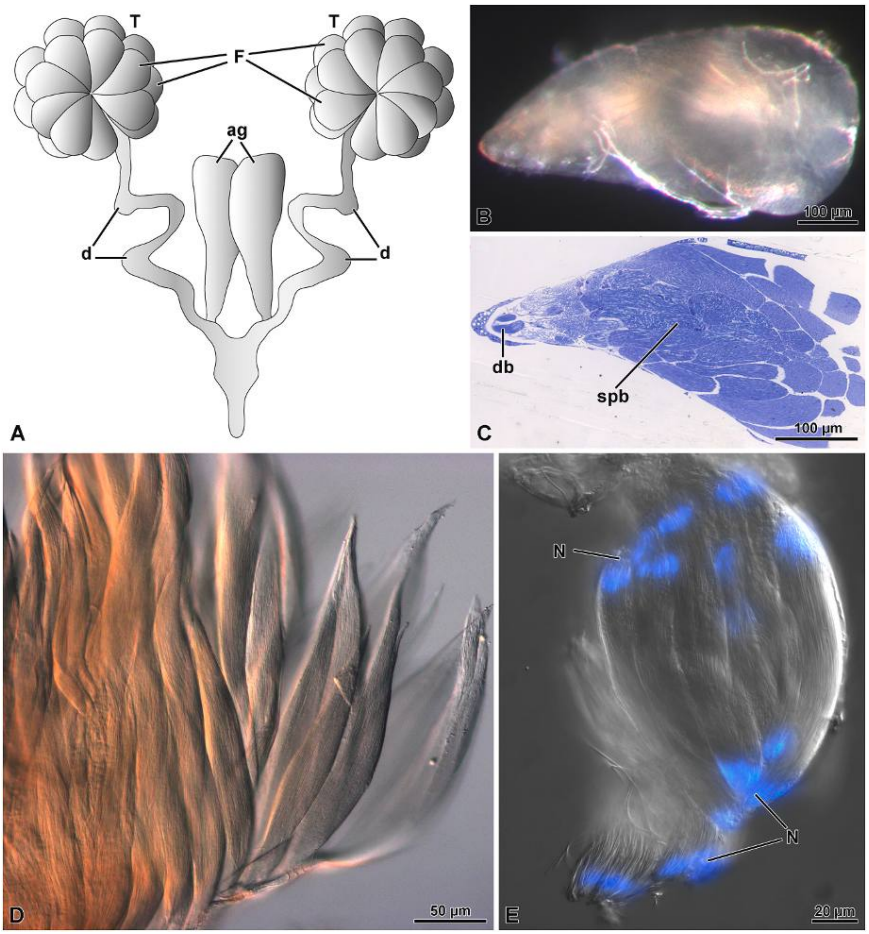

Fig. 5. *Mycetophagus quadripustulatus*. A) Schematic drawing of the male genital apparatus. ag accessory glands; D, deferent ducts; F, pyriform follicles; T, testes. B) The pyriform shape of a testis follicle. C) Semithin section of the pointed region of a follicle with the numerous sperm bundles (spb) and some dense bodies (db). D) A complex of elongated germ cysts in the testis follicle. E) Hoechst staining of some elongated sperm bundles showing the nucleus (N) at the two opposite extremities.

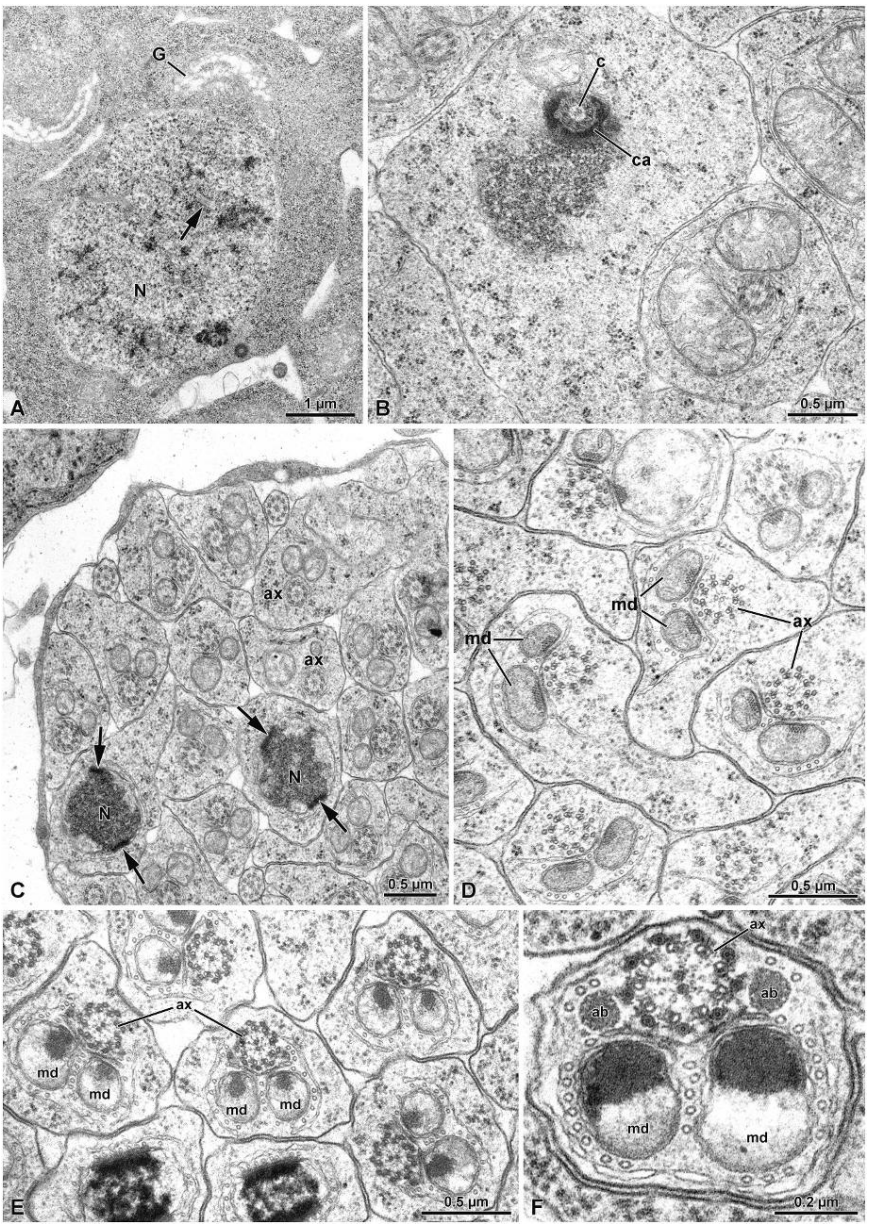

Fig. 6. *Mycetophagus quadripustulatus*. A) Cross section of a nucleus (N) of a spermatocyte with a synaptonemal complex (arrow). Note also the large Golgi apparatus (G). B) Cross section of the centriolar region (c) surrounded by the electron-dense material of the centriole adjunct (ca). C) Cross section of early spermatids with nucleus (N) showing chromatin condensation on both side (arrowheads). Some flagellar axonemes have a simple 9 + 2 organization (ax). D, E) Cross sections through two more developed spermatids with mitochondrial derivatives (md) showing crystallization of their matrix and a 9 + 9 + 2 flagellar axoneme (ax). F) Cross section of an almost mature spermatid showing the axoneme (ax) with electron-dense accessory tubules, two roundish accessory bodies (ab) and mitochondrial derivatives with a large area of matrix crystallized.

contains an inner perforatorium (Fig. 9C-E). The nucleus is also relatively short, measuring 7.0 µm, and has a cylindrical shape that tapers to a conical anterior extremity (Fig. 9C, E-H). Posteriorly, the nucleus contains a cavity 0.5 µm deep, which houses the axoneme on one side and a single mitochondrial derivative on the opposite side (Fig. 9E, G). The axoneme exhibits the typical 9 + 9 + 2 microtubular pattern with electron-dense accessory tubules. Next to the axoneme, two nearly equal elliptical mitochondrial derivatives are present (0.31 µm × 0.20 µm) (Fig. 9F). The accessory bodies are small and ovoid in cross section (62 nm wide) (Fig. 9F-G). Posteriorly, the mitochondrial derivatives decrease in size, and eventually only one remains for a short distance before disappearing (Fig. 9H). A cross section through the bundle in the deferent duct lumen reveal the opposite orientation of the flagellar axonemes, indicating that even in the deferent ducts the antiparallel arrangement of sperm is still evident (Fig. 9F). At the tail end, the axoneme loses its normal configuration, and the microtubular structures are no longer arranged in a regular array (Fig. 9I).

4. Discussion

In congruence with the molecular phylogenetic results proposed in Kergoat et al. (2014), McKenna et al. (2019) and Batelka et al. (2025a) Mycetophagidae seems to be related to Tetratomidae. At least *Mycetophagus quadripustulatus* and *Tetratoma fungorum*, the type species of the respective genera, share in the Central Europe the same microhabitat and bionomics. While Tenebrionidae is the most speciose family within

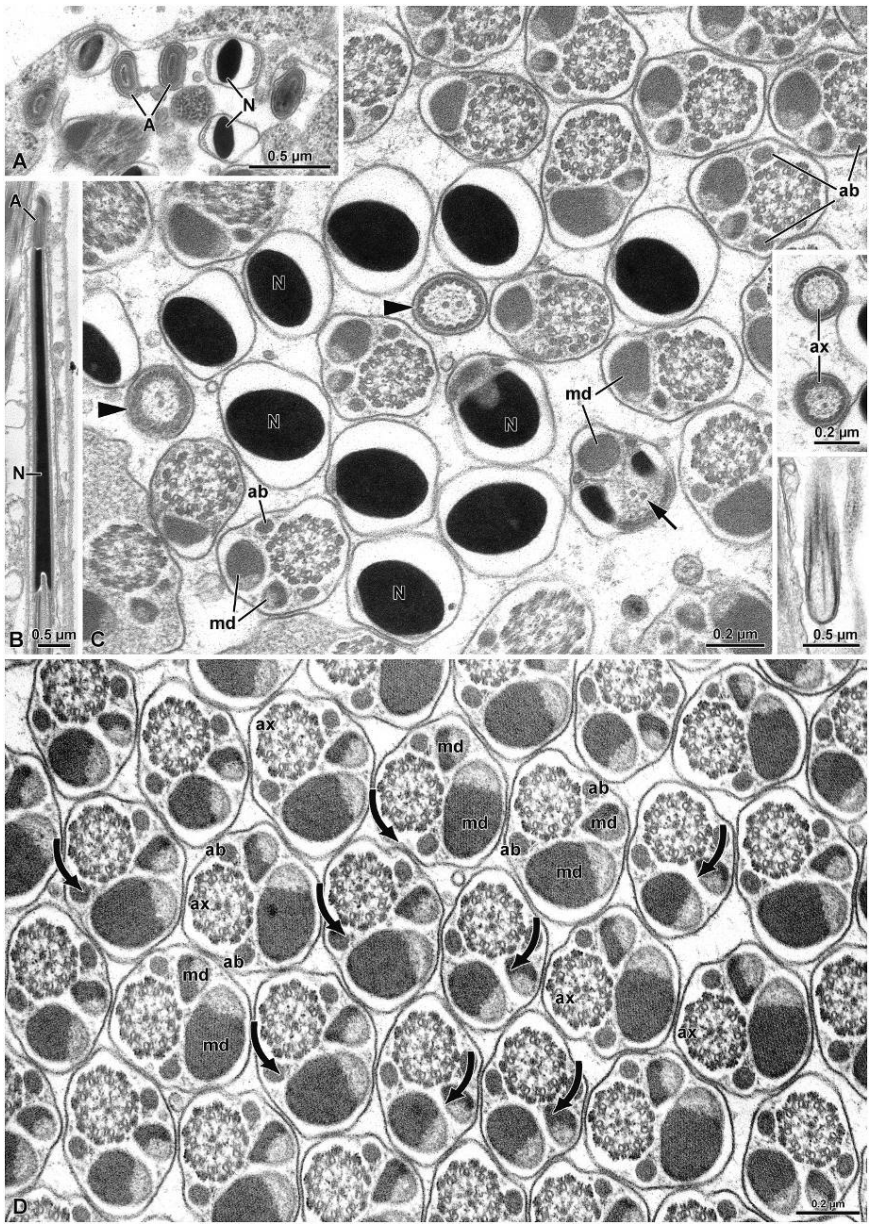

Fig. 7. *Mycetophagus quadripustulatus*. A) Cross section of the bilayered acrosome (A) and of the elliptical nuclear apex (N). B) Longitudinal section of the sperm head with the acrosome (A) and the nucleus (N). C) Cross section through the sperm bundle showing the posterior nuclear region (N) and the beginning of the flagellum. Note the nuclear remnants and the central tubules of the axoneme (arrows) on a side and a mitochondrial derivative (md) on the opposite side together with two small accessory bodies (ab). Two sections of the tail end are also visible (arrowheads). In the two insets the tail end is shown with the two central tubules and the microtubules beneath the plasma membrane. ax, axoneme. D) Cross section of the flagella at half sperm length. Axonemes have a different orientation due to the antiparallel position of the sperm bundles (see arrows). Note also the unequal size of the mitochondrial derivatives (md) and the two small accessory bodies (ab).

Tenebrionoidea, and comparable molecular data for *Neomida* and *Bolitophagus* are currently lacking, the two mycetophagous tenebrionids studied here are unrelated; *Neomida haemorrhoidalis* belongs to Diaperinae, whereas *Bolitophagus reticulatus* belongs to Tenebrioninae. Despite their phylogenetic distance, both species frequently co-occur in the same fruit bodies of *Fomes*.

The sperm ultrastructure of the four species studied here confirms previous findings regarding the main characteristics of Tenebrionoidea families (Baccetti et al., 1973; Dias et al., 2012, 2021, 2022a, b; Rezende et al., 2024a, b; Folly et al., 2021; Batelka et al., 2026), while also providing additional details useful for species identification. Excluding recently established Mordelloidea (with the crown families Mordellidae and Ripiphoridae), which exhibits unique morphological features (Dias et al., 2022a, b), Tenebrionoidea sensu Batelka et al. (2025b) share the unusual trait of having testes with germ cysts containing sperm arranged in an antiparallel orientation. This condition results from the migration of spermatid nuclei to opposite poles of the cyst during spermiogenesis (Dias et al., 2012) and is observed in *M. quadripustulatus*. At cyst maturity, sperm reach their final structure and are accommodated within the cyst volume by forming several flagellar loops, as seen in *B. reticulatus*, *N. haemorrhoidalis*, and *M. quadripustulatus*. Once mature, sperm are ready to exit the cysts and move toward the deferent ducts. In some species, after sperm have migrated to the deferent ducts and no new cysts develop, the testes may appear greatly reduced or absent. This may be the case in *T. fungorum*, where we did not find testes in the male genital apparatus but observed only long, large, and tortuous deferent

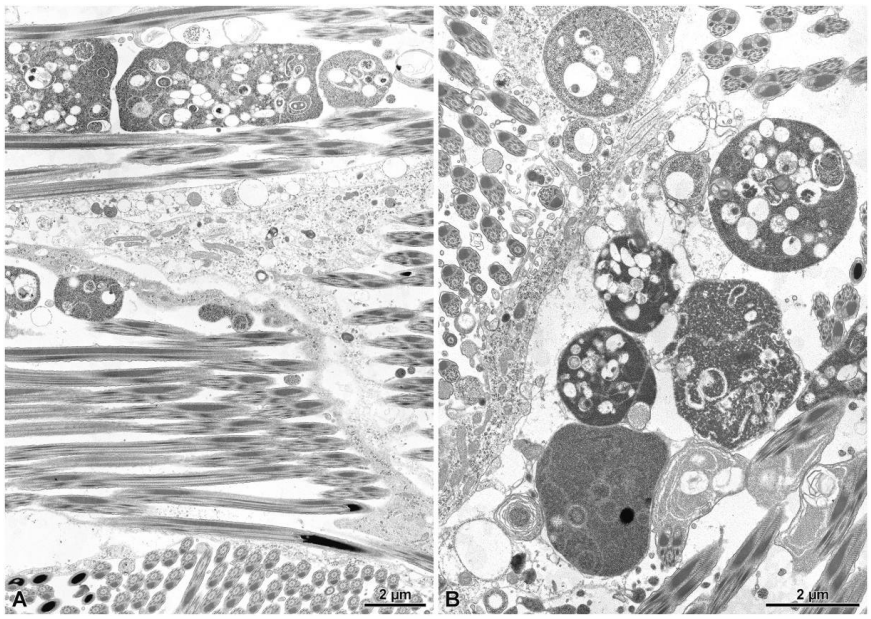

Fig. 8. *Mycetophagus quadripustulatus*. A, B) Cross sections through the pointed apex of a follicle showing large electron-dense bodies containing remnants of cyst cytoplasm intermingled with sperm bundles.

ducts filled with sperm. A similar situation was found in the ground beetle *Paussus favieri* (Gentile et al., 2026). The species examined in this study belong to three families - Tenebrionidae, Mycetophagidae, and Tetratomidae (see Table 1) - and are characterized by relatively long sperm, where measurable. This finding needs to be considered in future researches. However, sperm length is not comparable to that of Mordelloidea species (Dias et al., 2022a, b; Batelka et al., 2026), which have very long sperm contained in small cysts and thus forced to form flagellar loops. Comparative analysis of sperm characteristics revealed notable differences in acrosome length, such as the very short acrosome in *T. fungorum* (0.31 µm) compared to *N. haemorrhoidalis* (1.43 µm). Similarly, *B. reticulatus* has an acrosome 0.93 µm long, while *N. haemorrhoidalis* has an acrosome 1.43 µm long. The nuclei also differ significantly, with *N. haemorrhoidalis* having a nucleus more than three times longer (7.60 µm) than that of *B. reticulatus* (2.10 µm). Another Diaperinae species, *Phaleria testacea* (Rezende et al., 2024b), has a shorter acrosome and a longer nucleus compared to *N. haemorrhoidalis*. The lengths of the acrosome and nucleus also differ in the other two species examined: in *M. quadripustulatus* they are 0.82 µm and 5.70 µm, respectively, while *in T. fungorum* they are 0.31 µm and 7.0 µm. These data are not in agreement with those proposed by Kergoat et al. (2014), McKenna et al. (2019) and Batelka et al. (2025a) who recovered Mycetophagidae related to Tetratomidae. These data rather may be useful for species identification. The flagellar structure also shows remarkable differences. Similar shape and structure of the two mitochondrial derivatives were observed only in *T. fungorum*, a trait shared with several other Tenebrionoidea species (Baccetti et al., 1973; Nardi et al., 2013; Dias et al., 2012, 2013, 2015a, b, 2021, 2022a, b; Folly et al., 2021; Rezende et al., 2024a, b). In *B. reticulatus* and *M. quadripustulatus*, the left mitochondrial derivative is larger than the right, while in *N. haemorrhoidalis* the right derivative is larger. Whether these differences affect flagellar motility remains unclear and would require further investigation. The accessory bodies are generally small in all species examined, whereas in many Tenebrionoidea species they are larger and extend toward the axoneme to embrace it (Dias et al., 2021, 2022a, b). Notably, the accessory bodies of *Mylabris variabilis* and *M. hieracii* are very small and contain diffuse material along both sides of the axoneme (Dias et al., 2022a). The flagellar axoneme has the typical 9 + 9 + 2 microtubular structure with electron-dense accessory tubules. The structure of the tail end is also noteworthy. In insects, the flagellar end commonly displays disorganization of the orderly arrayed axonemes. This pattern is present only in *T. fungorum*, while in the other three species (*B. reticulatus*, *N. haemorrhoidalis*, and *M. quadripustulatus*), after the two central tubules terminate, all other microtubular structures, doublets, and accessory tubules move toward the periphery and align beneath the plasma membrane, forming a previously unobserved model. The data reported here on the sperm structure might be useful for establishing affinities among the examined species and will support further analyses of other unstudied species. However, it is clear that more species need to be studied before general conclusions about Tenebrionoidea and particularly Tenebrionidae can be drawn. The results obtained here, based on the sperm structure of a few species, nevertheless highlight the value of these characters for establishing relationships among the numerous species in the superfamily.

CRediT authorship contribution statement

Romano Dallai: Writing – review & editing, Writing – original draft, Supervision, Investigation, Conceptualization. **Pietro Lupetti:** Writing – review & editing, Writing – original draft, Supervision. **Mariangela Gentile:** Writing – review & editing, Writing – original draft, Investigation. **Jan Batelka:** Writing – review & editing, Writing – original draft, Resources. **David Mercati:** Writing – review & editing, Writing – original draft, Visualization, Investigation.

Declaration of Competing Interest

The authors declare that they have no known competing financial interests or personal relationships that could have appeared to influence the work reported in this paper.

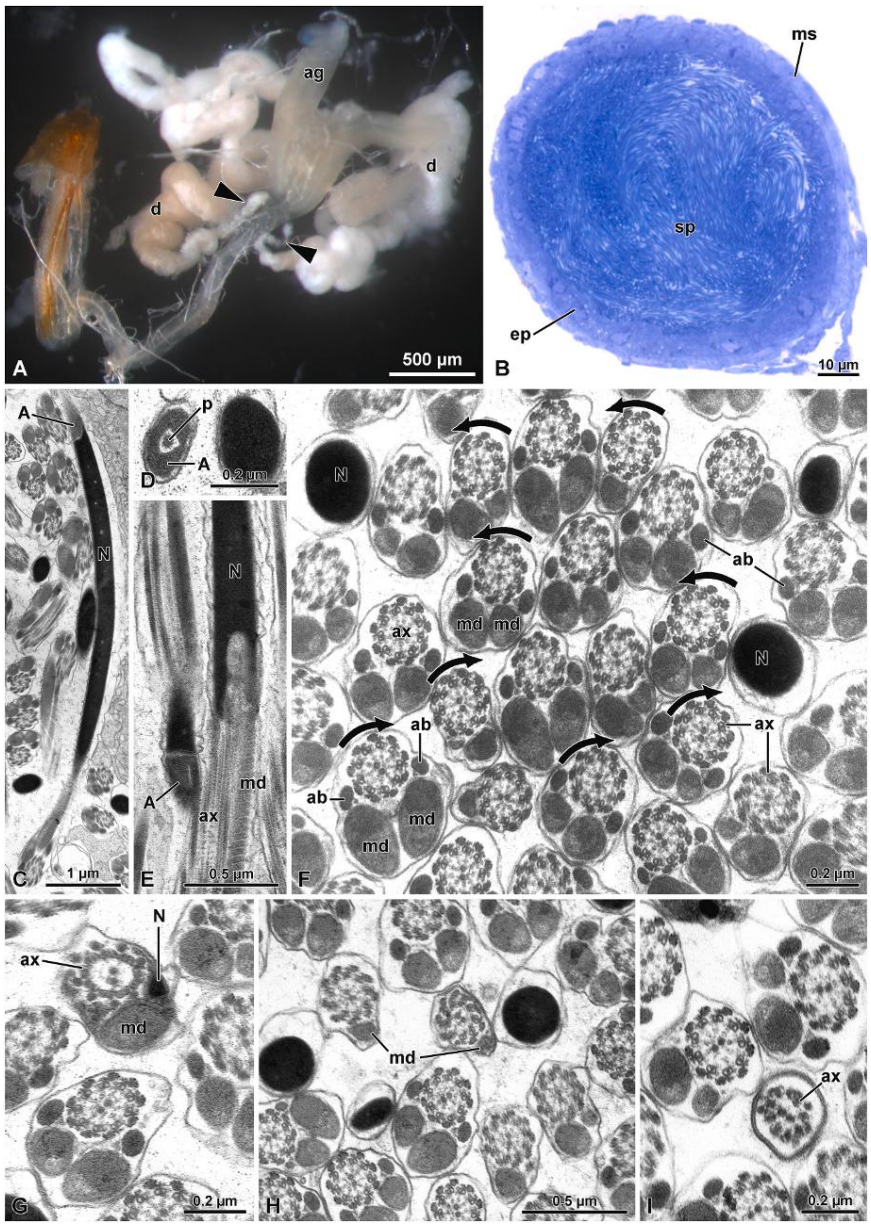

Fig. 9. *Tetratoma fungorum*. A) Male genital apparatus with long, large and sinuous deferent ducts (d). Note the apical extremities of these ducts where testes must be present (arrowheads). ag, accessory glands. B) Semithin cross section of a deferent duct filled with sperm (sp). ep, epithelium; ms, muscle layer. C) Longitudinal section of the sperm head with the short acrosome (A) and the almost cylindrical nucleus (N). D) Cross section of the acrosome (A) with the inner perforatorium (p). E) Longitudinal section of the nuclear posterior region (N). In the nuclear cavity the mitochondrial derivatives (md) and the flagellar axoneme (ax) are hosted. F) Cross section of sperm bundles with axonemes showing a different orientation due to the antiparallel position of the two bundles (see arrows). Note the almost equal mitochondrial derivatives (md), the axoneme (ax) and the ovoidal accessory bodies (ab). G) Cross section through the nuclear posterior end (N) with the beginning of the axoneme (ax) and one mitochondrial derivative (md). H, I) Cross sections of the tail end showing the reduced size and number of mitochondrial derivatives (md) and the axoneme disorganization (ax).

Table 1
Main characteristics of the sperm of the examined species

	Bolitophagus reticulatus	*Neomida haemorrhoidalis*	*Mycetophagus quadripustulatus*	*Tetratoma fungorum*
Family	Tenebrionidae		Mycetophagidae	Tetratomidae
Subfamily	Tenebrioninae	Diaperinae	Mycetophaginae	Tetratrominae
Total length	About 224 µm	About 180 µm		
Acrosome	0.93 µm + apical dense expansion	1.43 µm + apical empty expansion	0.82 µm	0.31 µm
Nucleus	2.10 µm	7.6 µm	5.7 µm	7 µm
Mitochondrial derivatives	Left mitochondria larger than the opposite	Right mitochondria larger than the opposite	Left mitochondria larger than the opposite	Similar
Accessory bodies	Large, elliptical	Small and globular or slightly elliptical	Small and globular or slightly elliptical	Small globular
Tail end	All microtubules beneath the plasma membrane	All microtubules beneath the plasma membrane	All microtubules beneath the plasma membrane	Disorganized axoneme

Data availability

No data was used for the research described in the article.

References

Afzelius, B.A., Dallai, R., 1994. Characteristics of the flagellar axoneme of Neuroptera, Coleoptera, and Strepsiptera. J. Morphol. 219, 15–20. https://doi.org/10.1002/jmor.1052190104.

Baccetti, B., Burrini, A.G., Dallai, R., Giusti, F., Mazzini, M., Renieri, T., Rosati, F., Selmi, G., 1973. Structure and function in the spermatozoon of *Tenebrio molitor*. The spermatozoon of Arthropoda XX. J. Mechanochem. Cell Motil. 2, 149–161.

Batelka, J. 2025b. Morphology, biology, evolution, and biodiversity of Ripiphoridae (Insecta: Coleoptera). PhD thesis. Charles University, Faculty of Science, Department of Zoology. Prague, 66 pp. ⟨https://dspace.cuni.cz/bitstream/handle/20.500.11956/205901/140138159.pdf?sequence=1⟩.

Batelka, J., Kundrata, R., Straka, J., 2025a. Phylogenomics and revised classification of Lymexyloidea and Tenebrionoidea (Coleoptera: Polyphaga: Cucujiformia). Syst. Entomol. 1–19. https://doi.org/10.1111/syen.12683.

Batelka, J., Mercati, D., Gentile, M., Lupetti, P., Dallai, R., 2026. The first comparison of the sperm ultrastructure of Lymexyloidea with Mordelloidea and Tenebrionoidea (Coleoptera). Arthropod Struct. Dev. 91, 1015407. https://doi.org/10.1016/j.asd.2026.101507.

Beutel, R.G., Friedrich, F., 2005. Comparative study of larvae of Tenebrionoidea (Coleoptera: Cucujiformia). Eur. J. Entomol. 102, 241–264. https://doi.org/10.14411/eje.2005.037.

Bouchard, P., Bousquet, Y., Aalbu, R.L., Alonso-Zarazaga, M.A., Merkl, O., Davies, A.E., 2021. Review of genus-group names in the family Tenebrionidae (Insecta, Coleoptera). ZooKeys 1050, 1-633. 10.3897/zookeys.1050.64217.

Cai, C., Tihelka, E., Giacomelli, M., Lawrence, J.F., Ślipiński, A., Kundrata, R., Yamamoto, S., Thayer, M.K., Newton, A.F., Leschen, R.A.B., Gimmel, M.L., Lü, L., Engel, M.S., Bouchard, P., Huang, D., Pisani, D., Donoghue, P.C.J. 2022. Integrated phylogenomics and fossil data illuminate the evolution of beetles. R. Soc. Open Sci. 9, 211771. https://doi.org/10.1098/rsos.211771.

Crowson, R.A., 1966. Observations on the constitution and subfamilies of the family Melandryidae (Coleoptera). Eos 41, 507–513.

Dallai, R., 2014. Overview on spermatogenesis and sperm structure of Hexapoda. Arthropod Struct. Dev. 43, 257–290. https://doi.org/10.1016/j.asd.2014.04.002.

Dias, G., Lino-Neto, J., Dallai, R., 2015b. The sperm ultrastructure of *Stictoleptura cordigera* (Füssli, 1775) (Insecta, Coleoptera, Cerambycidae). Tissue Cell 47, 73–77. https://doi.org/10.1016/j.tice.2014.11.007.

Dias, G., Lino-Neto, J., Mercati, D., Dallai, R., 2015a. The sperm ultrastructure and spermiogenesis of *Tribolium castaneum* (Coleoptera: Tenebrionidae) with evidence of cyst degeneration. Micron 73, 21–27. https://doi.org/10.1016/j.micron.2015.03.003.

Dias, G., Lino-Neto, J., Mercati, D., Fanciulli, P.P., Lupetti, P., Dallai, R., 2021. The sperm ultrastructure of *Pytho depressus* (Linnaeus, 1767) (Coleoptera, Pythidae). Micron 148, 103111. https://doi.org/10.1016/j.micron.2021.103111.

Dias, G., Lino-Neto, J., Mercati, D., Fanciulli, P.P., Lupetti, P., Dallai, R., 2022a. The sperm ultrastructure of members of basal Tenebrionoidea(Coleoptera). Arthropod Struct. Dev. 66, 101129. https://doi.org/10.1016/j.asd.2021.101129.

Dias, G., Mercati, D., Rezende, P.H., Lino-Neto, J., Fanciulli, P.P., Lupetti, P., Dallai, R., 2022b. New findings on the sperm structure of Tenebrionoidea (Insecta, Coleoptera). Insects 13, 485. https://doi.org/10.3390/insects13050485.

Dias, G., Oliveira, C.M., Lino-Neto, J., 2013. Sperm morphology and phylogeny of Lagriids (Coleoptera, Tenebrionidae). Arthropod Struct. Dev. 42, 379–384. https://doi.org/10.1016/j.asd.2013.04.002.

Dias, G., Yotoko, K.S.C., Gomes, L.F., Lino-Neto, J., 2012. Uncommon formation of two antiparallel sperm bundles per cyst in tenebrionid beetles (Coleoptera). Naturwissenschaften 99, 773–777. https://doi.org/10.1007/s00114-012-0949-6.

Folly, C., Pecci-Maddalena, I.S.C., Lopes-Andrade, C., Lino-Neto, J., 2021. The reproductive system of *Ceracis cornifer* (Mellié) and first description of sperm structure in a minute tree-fungus beetle (Tenebrionoidea: Ciidae). Arthropod Struct. Dev. 64, 101088. https://doi.org/10.1016/j.asd.2021.101088.

Gentile, M., Mercati, D., Brandmayr, P., Di Giulio, A., Lupetti, P., Dallai, R., 2026. Sperm morphology and ultrastructure in four species of ground beetles (Insects-Carabidae). Tissue Cell 101, 103403. https://doi.org/10.1016/j.tice.2026.103403.

Hu, Y.-J., Jia, F.-F., Hu, L., Wu, C., Tian, T., Li, T.-J., Chen, B., 2024. Comparative mitogenome research revealed the phylogenetics and evolution of the superfamily Tenebrionoidea (Coleoptera: Polyphage). Ecol. Evol. 14 (6), e11520. https://doi.org/10.1002/ece3.11520.

Jamieson, B.G.M., Dallai, R., Afzelius, B.A., 1999. Insects. Their Spermatozoa and Phylogeny. IBH Publishing Ltd, Oxford, p. 554.

Kergoat, G.J., Soldati, L., Clamens, A.-L., Jourdan, H., Jabbour-Zahab, R., Genson, G., Bouchard, P., Condamine, F.L., 2014. Higher level molecular phylogeny of darkling beetles (Coleoptera: Tenebrionidae). Syst. Entomol. 39, 486–499. https://doi.org/10.1111/syen.12065.

Lawrence, J.F., Newton, A.F., 1995. Families and subfamilies of Coleoptera with selected genera, notes, references, and data on family names. In: Biology, phylogeny, and classification of Coleoptera: papers celebrating the 80th birthday of R. A. Crowson. Pakaluk J., Ślipiński S.A (Eds.), Museum i Instytut Zoologii PAN, Warszawa. pp. 779–1006.

Lawrence, J.F., Ślipiński, A., Seago, A.E., Thayer, M.K., Newton, A.F., Marvaldi, A.E., 2011. Phylogeny of the Coleoptera based on morphological characters of adults and larvae. Ann. Zool. 61, 1–217. https://doi.org/10.3161/000345411X576725.

McKenna, D.D., Shin, S., Ahrens, D., Balke, M., Beza-Beza, C., Clarke, D.J., Donath, A., Escalona, H.E., Friedrich, F., Letsch, H., Liu, S., Maddison, D., Mayer, C., Misof, B., Murin, P.J., Niehuis, O., Peters, R.S., Podsiadlowski, L., Pohl, H., Scully, E.D., Yan, E. V., Zhou, X., Ślipiński, A., Beutel, R.G., 2019. The evolution and genomic basis of beetle diversity. Proc. Natl. Acad. Sci. USA 116, 24729–24737. https://doi.org/10.1073/pnas.1909655116.

Nardi, J.B., Delgado, J.A., Collantes, F., Miller, L.A., Bee, C.M., Kathirithamby, J., 2013. Sperm cells of a primitive Strepsipteran. Insects 4, 463–475. https://doi.org/10.3390/insects4030463.

Rezende, P.H., Mercati, D., Lupetti, P., Dallai, R., 2024a. The sperm structure of the Scraptiidae (Coleoptera; Tenebrionoidea. Micron 176, 103546. https://doi.org/10.1016/j.micron.2023.103546.

Rezende, P.H., da S. Paulo, M., Ayala-Costa, D., Texeira, A.G.P., Nascimento, F.W., Alves, M.P., Folly, C., Lino-Neto, J., Dias, G., 2024b. Evidence of antiparallel sperm bundles and limited sperm production in adult males of *Phaleria testacea* Say, 1824 (Tenebrionidae, Diaperinae). Tissue Cell 91, 102621. https://doi.org/10.1016/j.tice.2024.102621.

Robertson, J.A., Ślipiński, A., Moulton, M., Shockley, F.W., Giorgi, A., Lord, N.P., McKenna, D.D., Tomaszewska, W., Forrester, J., Miller, K.B., Whiting, M.F., McHugh, J.V., 2015. Phylogeny and classification of Cucujoidea and the recognition of a new superfamily Coccinelloidea (Coleoptera: Cucujiformia). Syst. Entomol. 40, 745–778. https://doi.org/10.1111/syen.12138.

Zhang, S.Q., Che, L.-H., Li, Y., Liang, D., Pang, H., Ślipiński, A., Zhang, P., 2018. Evolutionary history of Coleoptera revealed by extensive sampling of genes and species. Nat. Commun. 9, 205. https://doi.org/10.1038/s41467-017-02644-4.